

A novel 7 degrees of freedom model for upper limb kinematic reconstruction based on wearable sensors

Lorenzo Peppoloni¹ Alessandro Filippeschi² Emanuele Ruffaldi³ and Carlo Alberto Avizzano⁴

Abstract—Wearable motion tracking systems have gained large popularity in the last decades because of their effectiveness in many fields, from performance assessment to human-robot interaction. Among all the approaches, those based on inertial sensors have been widely explored. Since inertial sensors are affected by measurements drift, they need to be aided by other sensors, thus requiring sensor measurements to be fused. The most used sensor fusion techniques are based on Kalman filter. In particular, the Extended Kalman Filter (EKF) and the Unscented Kalman Filter (UKF) are used because of the non linearity characterizing most of the models. They often aim at reconstructing human motion by estimating limbs orientation, involving human’s kinematics to constrain relative motion of the limbs. These models often neglect part of the degrees of freedom (DoFs) that characterize human upper limbs, especially when modeling humerus motion with respect to the chest. In this paper we present a novel 7 DoFs model which represents a trade-off between modeling accuracy and complexity for the human upper limb. In particular, we model the human shoulder girdle taking into account also the humerus head’s elevation and the retraction due to the scapula’s and the clavicle’s motions. The model exploits inertial sensors measurements by means of an Unscented Kalman filter to reconstruct human movements. The system performance is validated firstly against a reconstruction based on an optical tracking system. Secondly, the 5 DoFs model extracted from the 7 DoFs one was checked to have state of the art performance and used to estimate the improvement of position estimation that are obtained by extending the model to 7 DoFs.

I. INTRODUCTION

Human motion reconstruction has been widely studied in the last decades because of its importance in several fields, from human performance assessment to health and rehabilitation applications. Traditional approaches to motion capture are based on optical methods: analysis of videotapes, marker-based motion capture of body landmarks and, recently, markerless techniques are example of such approaches. Although these systems can be very accurate in position estimation, all of them are very sensitive to lighting conditions and occlusions. Wearable sensors provide a smart alternative to optical systems, as they do not suffer from lighting and occlusions. Moreover, they do not require specific laboratory setups, thus allowing for being used outdoors. MEMS (microelectromechanical system) based inertial motion units

(IMU) are specifically successful in the wearable domain, as they are simple, unobtrusive, and self-contained. In their simplest form, they are composed of a gyroscope and an accelerometer (both biaxial or triaxial). Although IMUs are not afflicted by the problems of optical systems, they suffer from measurement drift phenomena, that make impossible to reconstruct motion by time integration of angular velocity and linear acceleration. To solve this issue, additional sensors (e.g. magnetometers, optical sensors, ultrawide band) that do not suffer from drift were added. Therefore, most of the motion reconstruction methods use sensor fusion techniques that allow also to take into account the kinematic constraints on the human limbs.

In this paper we focus on IMUs enhanced by triaxial magnetometers, that is the most common combination of sensors for IMU-based motion capture. This work focuses on a new model for reconstructing the upper limb motion. In particular, we propose a model of the shoulder kinematics that takes into account the humerus’ head elevation and profusion (both motions that do affect humerus orientation) in order to improve position estimation and track more complex movements. Therefore the proposed kinematics’ model has 7 DoFs, and it is an extension of the 5 DoFs models that are the most complex that we found in literature. Most of the systems that are available in literature validate their results against optical, marker-based techniques of motion reconstruction. We adopt the same technique as we will consider optical tracking motion reconstruction as ground truth and we will compare our results against it. Moreover, we implemented the corresponding 5 DoFs version of our model to assess the improvements that are obtained including further 2 DoFs. In summary, the main contributions of this work are: the introduction of a novel kinematic model for the human upper limb which better represents the shoulder girdle complex structure; the estimation of all the joint variables (angles, velocities and accelerations) for the body parts considered; a system performance assessment both for joint angles and wrist position, preserving joint angles estimation accuracy and improving position estimation w.r.t. the equivalent 5 DoFs model.

The paper is organized as follows. Section II provides an overview of the state of the art related to IMU-based motion reconstruction. Section III describes the methodology that we used, in particular the kinematic model and the state and measurements models. Section IV reports the experiments that we carried out to validate our model along with their results. Section V discusses the comparison of the results that we obtained with the proposed approach and other

¹ L. Peppoloni is with TECIP Institute, Scuola Superiore Sant’Anna, Italy l.peppoloni@sssup.it

² A. Filippeschi is with TECIP Institute, Scuola Superiore Sant’Anna, Italy a.filippeschi@sssup.it

³ E. Ruffaldi is with TECIP Institute, Scuola Superiore Sant’Anna, Italy e.ruffaldi@sssup.it

⁴ C.A. Avizzano is with TECIP Institute, Scuola Superiore Sant’Anna, Italy c.avizzano@sssup.it

state of the art approaches. Finally, the paper is closed by conclusions.

II. BACKGROUND

Works on human motion tracking can be grouped into two categories, according to their implementation of kinematic constraints:

- 1) *Separate estimation*: each limb's orientation is estimated as if it were disconnected from the others, after that kinematic constraints are eventually imposed to refine the estimation.
- 2) *Joint estimation*: human kinematics' constraints are embedded in a model that takes into account several (even all) the limbs at the same time.

There are several examples belonging to the first group. Yun and Bachmann [7] propose a double layer filtering approach. One layer is composed of the QUEST algorithm [5] that exploits acceleration and Earth's magnetic field data to estimate the quaternion representing limb orientation. The second layer is composed of an EKF that fuses the QUEST estimation with an orientation update based on the limb's angular velocity. The model used has 3 DoFs, for its validation each DoF estimation was compared to tilt table measurements. Zhou and Hu [10] present an orientation estimator based on Kalman filter. The filter estimation is the input of a kinematic model of human upper limbs (i.e. arm and forearm) to reconstruct the elbow and wrist positions. In this work the shoulder is assumed to be fixed. Zhang and Wu [9] use quaternions to represent the upper limbs orientation. It is estimated through a particle filter (PF) that implements the geometrical constraints of the elbow joint. Only one degree of freedom between upper arm and forearm is considered, obtaining less than 15° error in the angle estimation. Roetemberg et al. [3] propose a full body tracking system that is able to estimate 23 human limbs' orientations by integrating gyroscopes and accelerometers data. To correct their estimation, they also consider biomechanical characteristics of the human body. No performance assessment is given. Not considering the kinematics' constraints or separating them from the joint angles estimation may lead respectively to estimation distortions in the first case or to the development of so complex algorithms that were implemented for only 1 DoF.

The second possible approach consists on estimating joint variables of an upper limb kinematic model taken at the same time. Human limbs are considered to belong to a kinematic chain which models the geometrical constraints of the human skeleton. By exploiting this approach, Zhang et al. [8] obtained a 5 DoFs model for the human upper limb. The human shoulder is modeled as a spherical joint, while the forearm motion with respect to the upper arm is modeled through two rotational joints. An UKF is used to estimate joints angles and angular velocities. The authors obtain angles error of less than 2.86° for the upper arm and less than 12.60° for the forearm. This method does not show any estimation distortion if compared to the independent orientation estimation method. A similar approach is

proposed by El-Gohary and McNamara [1]. They present a 5 DoFs model for the human upper limbs, taking into account also angular accelerations. The estimation is done through an UKF filter, fusing on accelerometers and gyroscopes data. The obtained results are compared to optical tracking based ground truth data. The comparison shows an average root mean square error (RMSE) lower than 8° and a cross correlation coefficient $r \geq 0.95$ for the joint angles. Performance assessment for complex movements (more complex than involving 1 DoF at a time) is not reported. In particular, the estimation of the shoulder rotation angle and position assessments are not reported. Position accuracy is instead used by Mihelj [2] to validate his system. In this work the author presents an upper limb orientation estimation system. Each limb orientation is represented by a quaternion that is estimated taking into account the kinematic structure of the human skeleton. In this case also the wrist DoFs are included. The system performance is assessed both using an optical tracking system and an haptic interface to measure the wrist position. The system shows good performance both in the orientation and position tracking, but it does not calculate joint variables.

In contrast to the works described, this paper presents a high degrees of freedom model, which models the complex articulation of the human shoulder girdle with more accuracy. Joints variables (angles, velocities and accelerations) are estimated by fusing measurements from 3-axis gyroscopes, accelerometers and magnetometers through the use of an UKF. Differently from the listed works no assumptions are made on the motions to be tracked and all the degrees of freedom of the upper limb are estimated and reported as well as wrist position.

III. METHODOLOGY

Our model belongs to the joint estimation group. We exploited a kinematic model of the upper limbs to fuse joint angles estimation and IMUs measurements in an UKF, that has joint angles and their derivatives as state. Given the nonlinearity of some of the models we chose UKF as a trade-off between EKF and PF. Therefore we need three models for the joint angles estimation. The first is the model of upper limb kinematics, described in section III-A. The second, described in section III-B, provides the equations that model the state evolution over time, whereas the third model, that is shown in section III-C and is based on upper limbs kinematics, allow to write sensor measurements as function of the UKF state vector.

A. Kinematics Model

Several models can be identified for the upper limb. We follow the standard proposed by the International Society of Biomechanics (ISB) [6] with some simplifications. In particular we neglect few of the DoFs mentioned by ISB to limit the sensors' number and the algorithm complexity. We model upper limbs by taking the chest as root. We then suppose the clavicle to be linked to the chest by two revolute joints that model clavicle elevation/depression

Frame	a_i	α_i	d_i	ϑ_i	Joint
1	0	$\pi/2$	0	ϑ_1	Scapula Protraction
2	l_{cl}	$\pi/2$	0	ϑ_2	Scapula Elevation
3	0	$\pi/2$	0	ϑ_3	Shoulder Abduction
4	0	$\pi/2$	0	$\vartheta_4 - \pi/2$	Shoulder Rotation
5	l_{ua}	0	0	$\vartheta_5 + \pi/2$	Shoulder Flexion
6	0	$\pi/2$	0	$\vartheta_6 + \pi/2$	Elbow Flexion
7	0	0	l_{fa}	ϑ_7	Elbow Rotation

TABLE I

DH TABLE AND JOINT CORRESPONDENCE, l_{cl} , l_{ua} AND l_{fa} ARE CLAVICLE, UPPER ARM AND FOREARM LENGTH RESPECTIVELY.

and profusion/retraction. Then the humerus is supposed to have three rotational DoFs w.r.t. clavicle, i.e. shoulder abduction/adduction, internal rotation, and flexion/extension. Finally the forearm is supposed to have 2 rotational DoFs w.r.t. upper arm, respectively elbow flexion/extension and forearm pronation/supination.

We use the Denavit-Hartenberg convention to analytically write the kinematic chain, that we refer to as DH chain. According to this convention, a root frame τ_0 and one frame τ_i for each degree of freedom are introduced. Some of these frames are fixed to human limbs. In particular τ_0 is fixed w.r.t. the chest, τ_3 is fixed w.r.t. the humerus, and τ_5 is fixed w.r.t. the forearm. Each frame has its z_i axis aligned to the $i+1$ -th joint axis. Frames τ_{i-1} and τ_i are related each other by the $T_i^{i-1} \in \mathbb{R}^{4 \times 4}$ homogeneous matrix:

$$T_i^{i-1} = \begin{bmatrix} R_i^{i-1} & r_i^{i-1} \\ \mathbf{0}_{1,3} & 1 \end{bmatrix} \quad (1)$$

$$= \begin{bmatrix} c_{\vartheta_i} & -s_{\vartheta_i} c_{\alpha_i} & s_{\vartheta_i} s_{\alpha_i} & a_i c_{\vartheta_i} \\ s_{\vartheta_i} & c_{\vartheta_i} c_{\alpha_i} & -c_{\vartheta_i} s_{\alpha_i} & a_i s_{\vartheta_i} \\ 0 & s_{\alpha_i} & c_{\alpha_i} & d_i \\ 0 & 0 & 0 & 1 \end{bmatrix} \quad (2)$$

where rotation matrix R_i^{i-1} allows to align frames τ_{i-1} and τ_i axes, whereas r_i^{i-1} is the τ_i 's origin position in τ_{i-1} . The expanded expression of T_i^{i-1} is obtained when applying DH convention. In this latter matrix c_ψ and s_ψ are respectively $\cos(\psi)$ and $\sin(\psi)$. This matrix depends on four parameters, namely a_i , α_i , d_i , ϑ_i . The parameter d_i represents translation between frames τ_{i-1} and τ_i along z_{i-1} axis, ϑ_i the rotation around z_{i-1} axis necessary to align x_{i-1} and x_i , a_i is the translation along the x_i axis and, α_i the rotation around x_i axis to align z_{i-1} with z_i . Table I summarizes the parameters that define the kinematic chain of our kinematic model.

Three 3-axis inertial sensors, measuring angular velocity, linear acceleration and earth magnetic field, are used to reconstruct motion. Sensors frames' positions and orientations w.r.t. τ_0 are obtained by selecting a parent frame in the DH chain and then calculating the (constant) homogeneous matrix that relates the sensor's frame to the parent frame. The resulting kinematic structure for the left arm is shown in Figure 1.

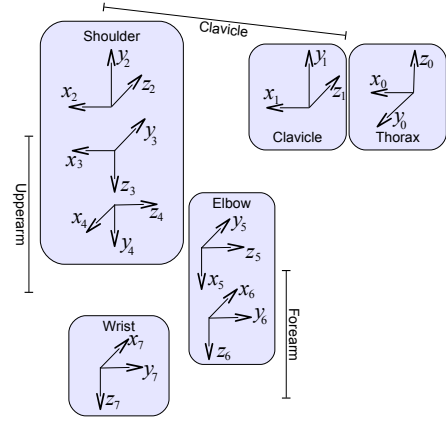


Fig. 1. Kinematic model of the left arm shown from behind. The model shows the reference frame in the thorax and the 7 moving frames of the kinematic model. As from the DH notation each frame T_i is expressed as a fixed transformations from T_{i-1} plus a rotation q_i along the axis T_i .

B. System Dynamics Model

Here we define the state space model of the UKF. To obtain a greater accuracy we include in the state model joint angles, velocities and accelerations, obtaining for each joint:

$$x_i = [\vartheta_i, \dot{\vartheta}_i, \ddot{\vartheta}_i]^T \quad i = 1, \dots, 7. \quad (3)$$

Given the generic formulation of the state space model, with additive noise for discrete systems:

$$x(k+1) = f(x(k)) + \nu_k \quad (4)$$

where $f(\cdot)$ is a nonlinear function and ν_k is the process Gaussian white noise, defining T_s the system sample time, the state model equations are:

$$\begin{aligned} \vartheta_i(k+1) &= \vartheta_i(k) + T_s \dot{\vartheta}_i(k) + \frac{1}{2} T_s^2 (\ddot{\vartheta}_i(k) + \nu_k) \\ \dot{\vartheta}_i(k+1) &= \dot{\vartheta}_i(k) + T_s (\ddot{\vartheta}_i(k) + \nu_k) \\ \ddot{\vartheta}_i(k+1) &= \ddot{\vartheta}_i(k) + \nu_k \end{aligned} \quad (5)$$

where the joint acceleration dynamic is modeled as a random walk process. The dynamic model considered leads to a linear state space representation where the dynamic matrix and the covariance matrix of the process for every joint are:

$$A_i = \begin{bmatrix} 1 & T_s & \frac{T_s^2}{2} \\ 0 & 1 & T_s \\ 0 & 0 & 1 \end{bmatrix} \quad Q_i = \begin{bmatrix} \frac{T_s^2}{2} \\ T_s \\ 1 \end{bmatrix} \begin{bmatrix} \frac{T_s^2}{2} & T_s & 1 \end{bmatrix}$$

C. Measurements Model

The measurements model describes how the state is related to the observed data. The general form of this model for a discrete system with additive noise is:

$$y(k) = h(x(k)) + \epsilon_k \quad (6)$$

where $h(\cdot)$ is a nonlinear function and ϵ_k is the white Gaussian noise on the measurements. In our case every sensor measures angular velocity (ω_s^s), linear acceleration (\ddot{x}_s^s) and magnetic field (m_s^s) in its own frame. Considering

the s^{th} IMU attached to the p^{th} (parent) frame we obtain the following measurements model:

$$\begin{aligned} \omega_s^s &= R_p^s(\omega_p^p + \dot{\vartheta}_{p+1}z_0) \\ \dot{x}_s^s &= R_p^s\dot{x}_p^p + S(\dot{\omega}_s^s)r_{p,s}^s + S(\omega_s^s)^2r_{p,s}^s + R_0^sg^0 \\ m_s^s &= R_0^sm^0 \end{aligned} \quad (7)$$

where R_p^s is the rotation matrix from parent frame to sensor frame, $S(v)$ is the skew-symmetric matrix from vector v , R_0^s is the rotation matrix from sensor to global frame, g^0 and m^0 are gravity and Earth magnetic field in the chest root frame, z_0 is the $(0, 0, 1)^T$ vector, and $r_{p,s}^s$ provides the position of sensor frame relative to parent in sensor frame. Equations in 7 are obtained according to Newton-Euler's formulation.

For those reasons we decided to use a UKF to estimate the system state.

D. Sensors Placement and Calibration

The three IMUs' placements aims at minimizing the muscle extrusive effect during movements. The first sensor was placed on the scapula beside the Angulus Acromialis, the second one on the lateral side of the upper arm above the elbow and the third was placed on the lateral side of the forearm a few centimeters far from the wrist. Sensor orientation is computed by means of an optimization process based on a simple calibration procedure: the subject is asked to hold his arm along the body (*n-pose*) and then perform a 90° shoulder abduction (*t-pose*). Sensors' orientations w.r.t. their parents are defined by three Euler angles, that are computed in this phase as solution of an optimization problem: the sought Euler's angles are the γ, β, ϕ angles that minimize the difference between the accelerometers' gravity measurements and the gravity vector in τ_0 . Therefore, for each sensor, said g^i the gravity vector in τ_i and τ_s the frame attached to the s -th sensor, the following problem is solved:

$$\min_{\gamma, \beta, \phi} \|R_0^s(\gamma, \beta, \phi)g^0 - \ddot{x}_s^s\| \quad (8)$$

since in static condition $\ddot{x}_s^s = g^s$.

Sensors translation parameters of the homogeneous matrix T_s^p are manually measured and provided as parameters. The same stands for the limbs lengths (l_{cl} , l_{ua} and l_{fa}). The same calibration process was carried out for both the 5 DoFs and 7 DoFs models. The position and orientation of the sensors w.r.t. the model kinematic is represented in Figure 2

IV. RESULTS

A. Experimental Setup

To assess our system performance we set up a twofold validation. Firstly joint angles estimation and landmarks position estimation performed by our 7 DoFs model is compared to an optical motion capture system that is considered as ground truth. Secondly the same comparison is carried out against an equivalent 5 DoFs model whose performance is at the state of the art. This is done to evaluate the accuracy of our approach in reconstructing kinematics, and to assess how much our approach allows to improve position estimation with respect to an equivalent 5 DoFs model that perform

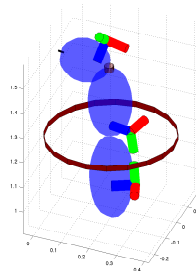


Fig. 2. Kinematic model of the arm, with the scapula, upper arm and lower arm shown as blue ellipsoids. The three sensor frames are shown using the color convention red-green-blue for the x-y-z axis. The figure shows also the variance of some of the joints depicted as a cylinder with a radius proportional to the variance.



Fig. 3. Experimental setup for synchronized IMUs and optical motion capture. Sensor frame with offset r_{off} from actual sensor frame origin and marker center in the magnified area.

at least as good as state of the art models. The Vicon motion capture system was used to gather ground truth data. Seven high resolution cameras (Vicon, MX+ 20) capture the subject motion. Nine reflective markers were placed on specific subject's body anatomical landmarks: clavicle; acromion; ulna trochlear notch and humerus throchlea axis; two markers to determine scaphoid-pisiform axis; one marker for each of the 3 IMU. Three 9-axis Invensense (Invensense, Borregas Ave Sunnyvale, CA, USA) MPU9150 IMUs were worn by the subject as described in section Methods III-D. Sensors data were sent via Bluetooth (version 2.0) to a central computing units at a rate of 100 Hz . We enabled the embedded algorithms from Invensense to filter magnetic disturbances. The model for kinematic reconstruction is implemented in Matlab Simulink[®] and it is run at 100 Hz frequency. The experimental setup is shown in Figure 3.

At the beginning of the experiment, the calibration procedure described in III-D was carried out. The participant was then asked to perform the following functional movements, exploring the possible joints space: elbow flexion/extension; forearm pronation/supination; shoulder abduction/adduction; shoulder rotation; shoulder flexion/extension; scapula anteposition/retroposition; scapula elevation/depression.

B. Estimation Results

1) *Joint angles comparison:* Joint angles $\tilde{\vartheta}_i$ were calculated from the optical data with a method adjusted from [4] to have ground truth data to be compared against our models estimations ϑ_i . Models were tested on a trial that is comparable for length and joint speed to the validation found in [1]. Figures 4, 5, and 6 show ϑ_i against $\tilde{\vartheta}_i$ for the

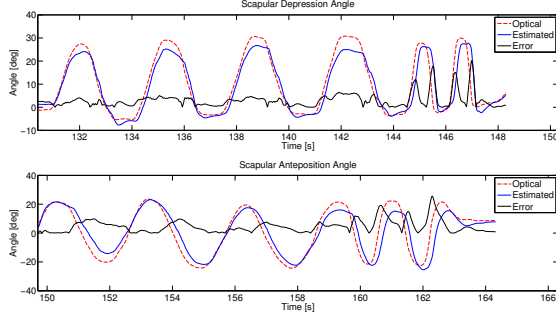


Fig. 4. Comparison of optical ($\tilde{\vartheta}_i$) and model based (ϑ_i) estimation for the scapular joints.

parts of the whole trial involving the functional movement that mostly stresses a given DoF.

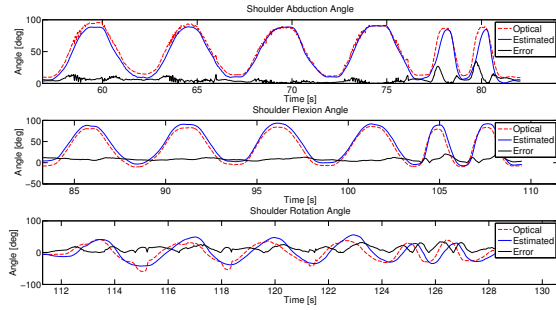


Fig. 5. Comparison of optical ($\tilde{\vartheta}_i$) and model based (ϑ_i) estimation for the shoulder joints.

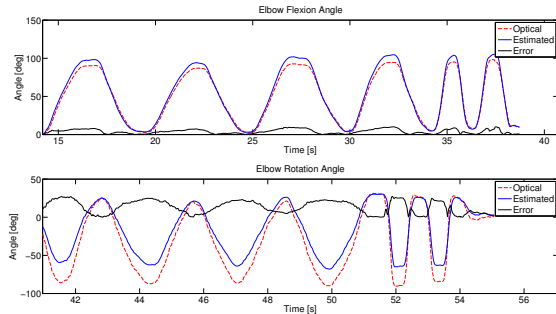


Fig. 6. Comparison of optical ($\tilde{\vartheta}_i$) and model based (ϑ_i) estimation for the elbow joints.

Models were assessed taking into account both the RMSE in joint angles ϑ_i estimation, namely $E_{\vartheta_i,k}$, and the cross-correlation coefficient of ϑ_i and $\tilde{\vartheta}_i$, called $C_{\vartheta_i,k}$ where k identifies the model.

Variable	$E_{\vartheta_i,5}$	$E_{\vartheta_i,7}$	$C_{\vartheta_i,5}$	$C_{\vartheta_i,7}$
ϑ_1	-	6.19	-	0.65
ϑ_2	-	3.43	-	0.74
ϑ_3	7.03	8.19	0.95	0.94
ϑ_4	6.03	10.68	0.87	0.63
ϑ_5	4.95	8.79	0.99	0.97
ϑ_6	9.93	5.00	0.98	0.99
ϑ_7	11.29	9.61	0.85	0.85
Average	7.85	7.41	0.93	0.82

TABLE II

RESULTS OF ESTIMATION. RMSES [DEG] AND CORRELATION ARE REPORTED FOR BOTH 5 DOFS AND 7 DOFS MODELS.

Variable	$E_{P_i,5}$	$E_{P_i,7}$	$C_{P_i,5}$	$C_{P_i,7}$
Shoulder	36.9	34.1	0.97	0.98
IMU arm	76.8	66.5	0.99	0.99
Elbow	70.6	65.5	0.98	0.98
IMU forearm	106.6	103.6	0.98	0.98
Average	72.7	67.4	0.98	0.98

TABLE III

RESULTS OF ESTIMATION. RMSES [MM] AND CORRELATION ARE REPORTED FOR BOTH 5 DOFS AND 7 DOFS MODELS.

We compared the trajectories of the optical markers on subject's shoulder, elbow and IMUs on upper arm and forearm with the ones estimated, for the same points, by our 7 DoFs model and by the equivalent 5 DoFs model. It is to be noted that the offset r_{off} between actual IMUs centers and the corresponding markers, shown in Figure 3, is taken into account in the model parameters. Figures 7, 8, 9 and 10 show the comparison among position estimations performed by the 5 DoFs model, the 7 DoFs model, and the optical tracking system.

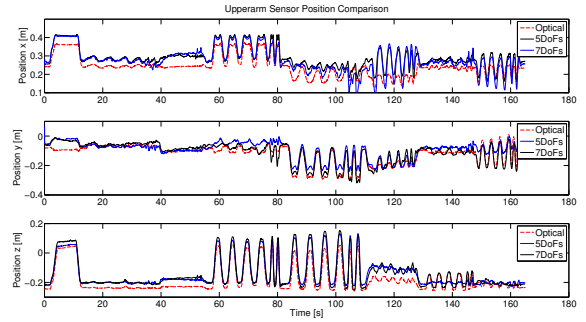


Fig. 7. Comparison of optical position and estimated positions (with 5 and 7 DoFs models) for upper arm sensor along each axis.

As for the joint angles we calculated, for each considered point, both the position error and the correlation of 5 DoFs and 7 DoFs with respect to the optical capture output. The comparison of the results is shown in table III.

V. DISCUSSION

The results of the experiment show that the system is capable to track joint angles with good results when compared

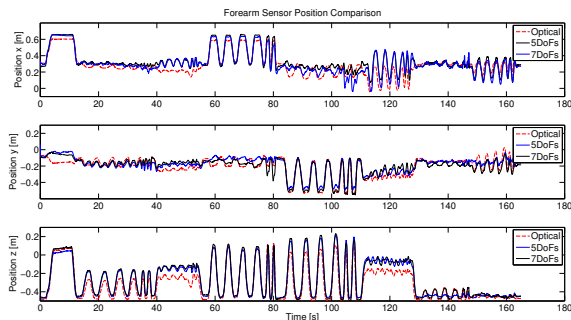


Fig. 8. Comparison of optical position and estimated positions (with 5 and 7 DoFs models) for forearm sensor along each axis.

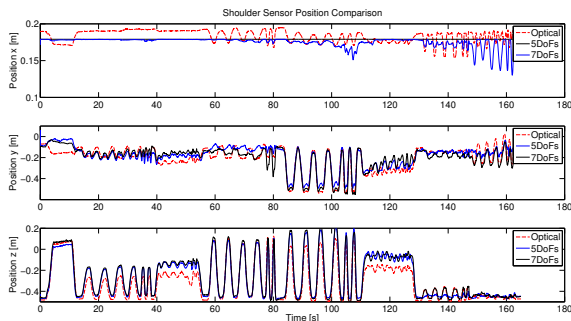


Fig. 9. Comparison of optical position and estimated positions (with 5 and 7 DoFs models) for subject's shoulder along each axis.

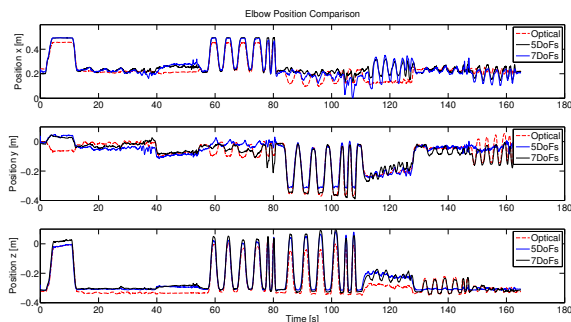


Fig. 10. Comparison of optical position and estimated positions (with 5 and 7 DoFs models) for subject's elbow along each axis.

to state of the art models. As a first achievement we can state that our model estimates joint angles slightly better than what reported by [1] for what regards joint angles that were considered in their models, and that the goodness of the estimation of clavicle angles is comparable to shoulder rotation and forearm pronation/supination. Although errors in optical estimation of joint angles and its alignment with our model estimation may have raised questions about the validation, the high values of correlation between model output and the optical estimation allow to conclude for the validity of the estimation.

Position estimation shows a slight improvement when using the 7 DoFs model with respect to the 5 DoFs model for what regards both error and correlation of model estimation

with respect to ground truth. The reason for the slightness of the improvement can be found in the position estimation comparison figures (more evident in Figure 9, but it can be found as well looking at the others). Although the 7DoFs model allows to better track clavicle motion, error in clavicle joint angles estimation cause part of this improvement to be lost by chance when comparing optical data against the constant estimation of 5DoF model. Therefore 7 DoFs model has still room for improvement in better clavicle IMU sensor placing and in model parameters estimation, whereas 5 DoFs model has smaller room for improvement and its shoulder position estimation is, of course, at its best.

As a final remark it is worth noting that the present system already works much faster than real-time in its Matlab-Simulink[®] implementation with recorded data. A C++ version has already been developed and preliminary tests show that it can run real-time on a Raspberry PI[®] board computer, thus being suitable for portable applications.

VI. CONCLUSION

We presented a novel 7 DoFs model that allows to reconstruct human upper limbs kinematics in terms of 2 DoFs motion of clavicle, 3 DoFs motion of the shoulder and 2 DoFs motion of the forearm with respect to the arm. The comparison against models that we cited in section II allowed to state that our 7 DoFs joint angle estimation is slightly better than the state of the art. Position estimation is better as well, therefore we conclude that, despite its simplicity, this model allows to track clavicle motion with sufficient precision, being a good starting point to tackle the problem of modeling shoulder motion.

REFERENCES

- [1] M. El-Gohary and J. McNames. Shoulder and elbow joint angle tracking with inertial sensors. *Biomedical Engineering, IEEE Transactions on*, 59(9):2635–2641, 2012.
- [2] M. Mihelj. Inverse kinematics of human arm based on multisensor data integration. *Journal of Intelligent and Robotic Systems*, 47(2):139–153, 2006.
- [3] D. Roetenberg, H. Luinge, and P. Slycke. Xsens mvn: full 6dof human motion tracking using miniature inertial sensors. Technical report, 2009.
- [4] D. Tolani, A. Goswami, and N. I. Badler. Real-time inverse kinematics techniques for anthropomorphic limbs. *Graphical models*, 62(5):353–388, 2000.
- [5] G. Wahba. A least squares estimate of satellite attitude. *Siam Review*, 7:409–409, 1965.
- [6] G. Wu, F. C. Van der Helm, H. Veeger, M. Makhsous, P. Van Roy, C. Anglin, J. Nagels, A. R. Karduna, K. McQuade, X. Wang, et al. Isb recommendation on definitions of joint coordinate systems of various joints for the reporting of human joint motionpart ii: shoulder, elbow, wrist and hand. *Journal of biomechanics*, 38(5):981–992, 2005.
- [7] X. Yun and E. R. Bachmann. Design, implementation, and experimental results of a quaternion-based kalman filter for human body motion tracking. *Robotics, IEEE Transactions on*, 22(6):1216–1227, 2006.
- [8] Z.-Q. Zhang, W.-C. Wong, and J.-K. Wu. Ubiquitous human upper-limb motion estimation using wearable sensors. *Information Technology in Biomedicine, IEEE Transactions on*, 15(4):513–521, 2011.
- [9] Z.-Q. Zhang and J.-K. Wu. A novel hierarchical information fusion method for three-dimensional upper limb motion estimation. *Instrumentation and Measurement, IEEE Transactions on*, 60(11):3709–3719, 2011.
- [10] H. Zhou and H. Hu. Reducing drifts in the inertial measurements of wrist and elbow positions. *Instrumentation and Measurement, IEEE Transactions on*, 59(3):575–585, 2010.